1 **Title Page**

2 Optimum growth temperature declines with body size within fish species

3

4 Max Lindmark[a,1], Jan Ohlberger[b], Anna Gårdmark[c]

5

6 [a] Swedish University of Agricultural Sciences, Department of Aquatic Resources, Institute of

7 Coastal Research, Skolgatan 6, Öregrund 742 42, Sweden

8 [b] School of Aquatic and Fishery Sciences (SAFS), University of Washington, Box 355020, Seattle,

9 WA 98195-5020, USA

10 [c] Swedish University of Agricultural Sciences, Department of Aquatic Resources, Skolgatan 6,

11 SE-742 42 Öregrund, Sweden

12

13 [1] Author to whom correspondence should be addressed. Current address:

14 Max Lindmark, Swedish University of Agricultural Sciences, Department of Aquatic Resources,

15 Institute of Marine Research, Turistgatan 5, Lysekil 453 30, Sweden, Tel.: +46(0)104784137,

16 **email**: max.lindmark@slu.se

17

18 **Keywords**: body growth, metabolic rate, consumption rate, temperature-size rule, metabolic

19 theory of ecology

20

21

22

23

Abstract

According to the temperature-size rule, warming of aquatic ecosystems is generally predicted to increase individual growth rates but reduce asymptotic body sizes of ectotherms. However, we lack a comprehensive understanding of how growth and key processes affecting it, such as consumption and metabolism, depend on both temperature and body mass within species. This limits our ability to inform growth models, link experimental data to observed growth patterns, and advance mechanistic food web models. To examine the combined effects of body size and temperature on individual growth, as well as the link between maximum consumption, metabolism and body growth, we conducted a systematic review and compiled experimental data on fishes from 59 studies that combined body mass and temperature treatments. By fitting hierarchical models accounting for variation between species, we estimated how these three processes scale jointly with temperature and body mass within species. We found that whole-organism maximum consumption increases more slowly with body mass than metabolism, and is unimodal over the full temperature range, which leads to the prediction that optimum growth temperatures decline with body size. Using an independent dataset, we confirmed this negative relationship between optimum growth temperature and size within fish species. Small individuals may therefore exhibit increased growth with initial warming, whereas larger conspecifics could be the first to experience negative impacts of warming on growth. These findings help advance mechanistic models of individual growth and food web dynamics and improve our understanding of how climate warming affects the growth and size structure of aquatic ectotherms.

Introduction

47

48   Individual body growth is a fundamental process powered by metabolism, and thus depends on

49   body size and temperature (Brown *et al.* 2004). It affects individual fitness and life history traits,

50   such as maturation size, population growth rates (Savage *et al.* 2004), and ultimately energy

51   transfer across trophic levels (Andersen *et al.* 2009; Barneche & Allen 2018). Therefore,

52   understanding how growth scales with body size and temperature is important for predicting the

53   impacts of global warming on the structure and functioning of ecosystems.

54   Global warming is predicted to lead to declining body sizes of organisms (Daufresne *et al.*

55   2009; Gardner *et al.* 2011). The temperature size-rule ('TSR') states that warmer rearing

56   temperatures lead to faster developmental times (and larger initial size-at-age or size-at-life-stage),

57   but smaller adult body sizes in ectotherms (Atkinson 1994; Ohlberger 2013). This relationship is

58   found in numerous experimental studies (Atkinson 1994), is reflected in latitudinal gradients

59   (Horne *et al.* 2015), and is stronger in aquatic than terrestrial organisms (Forster *et al.* 2012; Horne

60   *et al.* 2015). Support for the TSR exists in fishes, in particular in young fish, where reconstructed

61   individual growth histories often reveal positive correlations between growth rates and temperature

62   in natural systems (Thresher *et al.* 2007; Neuheimer *et al.* 2011; Baudron *et al.* 2014; Huss *et al.*

63   2019). However, whether the positive effect of warming on growth is indeed limited to small

64   individuals within a species, as predicted by the temperature size-rule, is less clear. Negative

65   correlations between maximum size, asymptotic size or size-at-age of old fish and temperature

66   have been found in commercially exploited fish species (Baudron *et al.* 2014; van Rijn *et al.* 2017;

67   Ikpewe *et al.* 2020). However, other studies, including large scale experiments, controlled

68   experiments and latitudinal studies or observational data on unexploited species, have found no or

69   less clear negative relationships between maximum size, growth of old fish or mean size and

70   temperature (Barneche *et al.* 2019; Huss *et al.* 2019; Van Dorst *et al.* 2019; Audzijonyte *et al.*

71   2020; Denderen *et al.* 2020) and differences between species may be related to life history traits

72   and depend on local environmental conditions (Denderen *et al.* 2020; Wang *et al.* 2020).

73   While the support for TSR is mixed, and the underlying mechanisms are not well understood

74   (Ohlberger 2013; Audzijonyte *et al.* 2019; Neubauer & Andersen 2019), theoretical growth

75   models, such as Pütter growth models (Pütter 1920), including the von Bertalanffy growth model

76   (VBGM) (von Bertalanffy 1957), commonly predict declines in asymptotic body mass with

77   temperature and declines in optimum growth temperature with body mass, in line with the TSR

78   (Perrin 1995; Morita *et al.* 2010; Pauly & Cheung 2018b; Pauly 2021). Yet, the physiological basis

79   of these models has been questioned, as the commonly applied scaling parameters (mass

80   exponents) tend to differ from empirical estimates (Lefevre *et al.* 2018; Marshall & White 2019).

81   Hence, despite attempting to describe growth from first principles, Pütter growth models can also

82   be viewed as phenomenological. In more mechanistic growth models, the difference between

83   energy gain and expenditure is partitioned between somatic growth and gonads (Ursin 1967;

84   Kitchell *et al.* 1977; Jobling 1997; Essington *et al.* 2001). Energy gain is normally the amount of

85   energy extracted from consumed food and expenditure, which is defined as maintenance, activity

86   and feeding metabolism. These components of the energetics of growth are found in dynamic

87   energy budget models (Kitchell *et al.* 1977; Kooijman 1993), including those used in

88   physiologically structured population models (PSPMs) (de Roos & Persson 2001) and size-

89   spectrum models (Hartvig *et al.* 2011; Maury & Poggiale 2013; Blanchard *et al.* 2017). Therefore,

90   it is important to understand how consumption and metabolism rates scale with body mass and

91   temperature in order to understand if and how growth of large fish within populations is limited

92   by temperature, and to evaluate the physiological basis of growth models.

93   Moreover, the effect of body mass and temperature on growth dynamics should be evaluated

94   over ontogeny at the intraspecific level (within species), which better represents the underlying

95   process than interspecific data (among species) (Marshall & White 2019). For instance, we do not

96   expect an interspecific relationship between optimum growth temperature and body mass, but

97   within species it may have a large effect on growth dynamics. Despite this, intraspecific body mass

98   and temperature scaling is often inferred from interspecific data, and we know surprisingly little

99   about average relationship between consumption and metabolic exponents within species

100   (Marshall & White 2019). Importantly, how physiological rates depend on mass and temperature

101   within species can differ from the same relationships across species (Glazier 2005; Rall *et al.* 2012;

102   Jerde *et al.* 2019). Across species, rates are often assumed and found to scale as power functions

103   of mass with exponents of 3/4 for whole organism rates, exponentially with temperature, and with

104   independent mass and temperature effects (e.g., in the Arrhenius fractal supply model (AFS)

105   applied in the metabolic theory of ecology, MTE (Gillooly *et al.* 2001; Brown *et al.* 2004; Downs

106   *et al.* 2008)). In contrast, within species, deviations from a general 3/4 mass exponent are common

107   (Clarke & Johnston 1999; Bokma 2004; Barneche *et al.* 2019; Jerde *et al.* 2019), rates are typically

108   unimodally related to temperature and activation energies can vary a lot (Dell *et al.* 2011; Englund

109   *et al.* 2011; Rall *et al.* 2012; Pawar *et al.* 2016; Uiterwaal & DeLong 2020) and the effects of mass

110   and temperature can be interactive (Xie & Sun 1990; Glazier 2005; García García *et al.* 2011;

111   Ohlberger *et al.* 2012; Lindmark *et al.* 2018) (but see Jerde *et al*. (2019)). Extensions of the MTE

112   include fitting multiple regression models where coefficients for mass and temperature are

113   estimated jointly (Downs *et al.* 2008), as well as fitting non-linear models that can capture the de-

114   activation of biological rates at higher temperatures (Schoolfield *et al.* 1981; Dell *et al.* 2011;

115   Englund *et al.* 2011; Padfield *et al.* 2017). To advance our understanding of the intraspecific

116   properties of mass- and temperature dependence of biological rates, intraspecific data with

117   variation in both mass and temperature are needed.

118   In this study, we analyzed how maximum consumption, metabolism and growth rate of fish

119   scale intraspecifically with mass and temperature. We performed a systematic literature review by

120   searching the Web of Science Core Collection to compile datasets on individual-level maximum

121   consumption, metabolism and growth rates of fish from experiments in which the effect of fish

122   body mass is replicated across multiple temperatures within species (total n=3672, with data from

123   13, 20 and 34 species for each rate, respectively). We then fit hierarchical Bayesian models to

124   estimate general intraspecific scaling parameters while accounting for variation between species.

125   The estimated mass dependence and temperature sensitivity of consumption and metabolism were

126   used to quantify average changes in net energy gain (and hence, growth, assumed proportional to

127   net energy gain) over temperature and body mass. Lastly, we compared our predicted changes in

128   optimum growth temperature over body mass with an independent experimental dataset on

129   optimum growth temperatures across individuals of different sizes within species.

130

131   **Results**

132   We identified that within species of fish, metabolic rates increase faster with body mass than

133   maximum consumption rates, and neither of these rates conform to the commonly predicted 3/4

134   scaling with body mass (Fig. 1). We also quantified the unimodal relationship of consumption rate

135   over the full temperature range (Fig. 2). Combined, these scaling relationships lead to the

136   prediction, based on Pütter-type growth models, that optimum growth temperature declines with

137   body size (Fig. 3). The prediction of declining optimum growth temperatures with size was

138   confirmed by our analysis of independent experimental growth rate data. We find that within

139   species the optimum growth temperature declines with body size by 0.31°C per unit increase in the

140   natural log of relative body mass (Fig. 4). Below we present the underlying results in more detail.

141   We found that the average intraspecific mass exponent for consumption rate is smaller (0.63

142   [0.55, 0.71]) than that for metabolic rate (0.79 [0.74, 0.84]), based on the non-overlapping

143   Bayesian 95% credible intervals (Fig. 1). It is also probable that the scaling exponents differ from

144   3/4 (that is predicted by the MTE), because >99% of the posterior distribution of the mass exponent

145   of maximum consumption is below 3/4, and 95% of the posterior distribution of the mass exponent

146   of metabolic rate is above 3/4. Activation energies of maximum consumption rate and metabolism

147   are both similar (0.69 [0.54, 0.85] and 0.62 [0.57, 0.67] respectively; Fig. 1) and largely fall within

148   the prediction from the MTE (0.6-0.7 eV) (Brown *et al.* 2004). The global intraspecific intercept

149   for routine and resting metabolic rate is estimated to be 1.85 [1.68, 2.04], and for standard

150   metabolic rate it is 1.29 [0.97, 1.61] (*SI Appendix,* Fig. S7). Models where all coefficients varied

151   by species were favored in terms of WAIC (M5 and M1, for consumption and metabolism,

152   respectively) (*SI Appendix*, Table S4). We found statistical support for a species-varying mass and

153   temperature interaction for metabolic rate; 98% of the posterior distribution of the global

154   interaction coefficient μ_{β_3} is above 0 (*SI Appendix,* Fig. S5). The estimated coefficient is 0.0018

155   [0.015, 0.037] on the Arrhenius temperature scale, which corresponds to a decline in the mass

156   scaling exponent of metabolic rate by 0.0026 $°C^{-1}$. The selected model for maximum consumption

157   rate did not include an interaction term between mass and temperature (M5).

158   We estimated the parameters of the Sharpe-Schoolfield equation (Eq. 4) for temperature-

159   dependence of consumption including data beyond peak temperature as: activation energy, E_j =

160   0.73 [0.54, 0.94], rate at reference temperature, C_{0_j} = 0.79 [0.58, 0.99], temperature at which the

161   rate is reduced to half (of the rate in the absence of deactivation) due to high temperatures, T_h =

162   0.75 [-0.86, 2.37], and the rate of the decline past the peak, $E_h = 1.89$ [1.68, 2.1]. This shows that

163   the relationship between consumption rate and temperature is unimodal and asymmetric, where

164   the decline in consumption rate at high temperatures is steeper than the increase at low

165   temperatures (Fig. 2).

166   The above results provide empirical support for the two criteria outlined in Morita et al., (2010)

167   that result in declining optimum temperatures with size, i.e. (i) smaller whole organism mass

168   exponent for consumption than metabolism (Fig. 1) and (ii) that growth reaches an optimum over

169   temperature. In our case, the second criterion is met because consumption reaches a peak over

170   temperature (Fig. 2) (in contrast to Morita *et al*. (2010), who assumed consumption to be linearly

171   related to temperature, based on data from Atkinson (1994)). We illustrate the consequence of

172   these findings in Fig. 3, which shows that the optimum temperature for net energy gain is reached

173   at a lower temperature for a larger fish because of the difference in mass exponents of consumption

174   and metabolism and because consumption is unimodally related to temperature. Assuming growth

175   is proportional to net energy gain, this predicts that optimum growth temperature declines with

176   body size.

177   Using independent data from growth trials across a range of body sizes and temperatures, we

178   also find strong statistical support for a decline in optimum growth temperature with body mass

179   within species, because 92% of the posterior density of the global slope estimate (μ_{β_1}) is below 0.

180   The models with and without species-varying slopes were indistinguishable in terms of WAIC (*SI*

181   *Appendix*, Table S5), and we present the results for the species-varying intercept and slope model,

182   due to slightly better model diagnostics (*SI Appendix*, Fig. S24-27). The global relationship is

183   given by the model: $T_{opt} = -0.074 - 0.31 \times m$, where m is the natural log of the rescaled body

184   mass, calculated as the species-specific ratio of mass to maturation mass.

185

Discussion

187   In this study, we systematically analyzed the intraspecific scaling of consumption, metabolism and

188   growth with body mass and temperature. We found strong evidence for declining optimum growth

189   temperatures as individuals grow in size, based on two independent approaches. First, we find

190   differences in the intraspecific mass-scaling of consumption and metabolism, and a unimodal

191   temperature dependence of consumption, which lead to predicted declines in optimum temperature

192   for net energy gain (and hence growth) with size. Second, we confirm this prediction using

193   intraspecific growth rate data of fish from temperature experiments. Our analysis thus

194   demonstrates the importance of understanding intraspecific scaling relationships when predicting

195   responses of fish populations to climate warming.

196   That warming increases growth and development rates but reduces maximum or adult size is

197   well known from experimental studies, also referred to as the temperature-size rule (TSR). Yet,

198   the mechanisms underlying the TSR remain poorly understood. Pütter-type growth models,

199   including the von Bertalanffy growth equation (VBGE), predict that the asymptotic size declines

200   with warming if the ratio of the coefficients for energy gains and losses (H/K in Eq. 7) (Pauly &

201   Cheung 2018b) declines with temperature. However, the assumptions underlying the VBGE were

202   recently questioned because of the lack of empirical basis for the scaling exponents and the effects

203   of those on the predicted effects of temperature on asymptotic size (Lefevre *et al.* 2018; Marshall

204   & White 2019). Specifically, the allometric exponent of energy gains (a) is assumed to be smaller

205   than that of energetic costs (b) (Eq. 7). This is based on the assumption that anabolism scales with

206   the same power as surfaces to volumes ($a = 2/3$) and catabolism, or maintenance metabolism, is

207   proportional to body mass ($b = 1$) (von Bertalanffy 1957; Pauly & Cheung 2018a). In contrast,

208   maintenance costs are commonly thought to instead be proportional to standard metabolic rate,

209   which in turn often is proportional to intake rates at the interspecific level (Brown *et al.* 2004;

210   Marshall & White 2019). This leads to $a \approx b$, resulting in unrealistic growth trajectories and

211   temperature dependencies of growth dynamics in Pütter models (Lefevre *et al.* 2018; Marshall &

212   White 2019). However, similar to how the existence of large fishes in tropical waters does not

213   invalidate the hypothesis that old individuals of large-bodied fish may reach smaller sizes with

214   warming, interspecific scaling parameters cannot reject or support these model predictions on

215   growth *within* species. We show that the average intraspecific whole-organism mass scaling

216   exponent of metabolism is larger than that of maximum consumption, i.e., the inequality $a < b$

217   holds at the intraspecific level. By contrast, Pawar *et al.* (2012) estimated larger mass exponents

218   for consumption than metabolic rate (0.84 and 1.04 in 2D and 3D foraging) from interspecific data,

219   which reveals the importance of parameterizing processes occurring over ontogeny with

220   intraspecific rather than interspecific data. When accounting for the smaller intraspecific mass

221   exponent of consumption, and the unimodal thermal response of consumption, the thermal

222   response of net energy gain is characterized by the optimum temperature being a function of body

223   size (Morita *et al.* 2010). Therefore, empirically derived intraspecific parameterizations of simple

224   growth models result in predictions in line with the TSR, in this case via declines in optimum

225   growth temperatures over ontogeny rather than declines in asymptotic sizes.

226   Declines in optimum growth temperatures over ontogeny as a mechanism for TSR-like growth

227   dynamics do not rely on the assumption that the ratio of the coefficients for energy gains and losses

228   declines with temperature. In fact, we find that when using data from sub-peak temperatures only,

229   the average intraspecific predictions about the activation energy of metabolism and consumption

230   do not differ substantially, which implies there is no clear loss or gain of energetic efficiency with

231   warming within species below temperature optima. This is in contrast to other studies, e.g.

232   Lemoine & Burkepile (2012) and Rall *et al.* (2010). However, it is in line with the finding that

233   growth rates increase with temperature (e.g. Angilletta & Dunham 2003), which is difficult to

234   reconcile from a bioenergetics perspective if warming always reduced net energy gain. Our

235   analysis instead suggests that the mismatch between gains and losses occurs when accounting for

236   unimodal consumption rates over temperature. The match, or mismatch, between the temperature

237   dependence of feeding vs. metabolic rates is a central question in ecology that extends from

238   experiments to meta-analyses to food web models (Vasseur & McCann 2005; Rall *et al.* 2010;

239   Lemoine & Burkepile 2012; Fussmann *et al.* 2014; Lindmark *et al.* 2019). Our study highlights

240   the importance of accounting for non-linear thermal responses for two main reasons. First, the

241   thermal response of net energy gain reaches a peak at temperatures below the peak for

242   consumption. Secondly, as initial warming commonly leads to increased growth rates, the effect

243   of warming on growth rates depends on temperature, and growth should therefore not be assumed

244   to be monotonically related to temperature.

245   Life-stage dependent optimum growth temperatures have previously been suggested as a

246   component of the TSR (Ohlberger 2013). Although previous studies have found declines in

247   optimum growth temperatures with body size in some species of fishes and other aquatic

248   ectotherms (Wyban *et al.* 1995; Panov & McQueen 1998; Steinarsson & Imsland 2003; Björnsson

249   *et al.* 2007; Handeland *et al.* 2008), others have not (Brett *et al.* 1969; Elliott & Hurley 1995).

250   Using systematically collated growth data from experiments with variation in both size and

251   temperature treatments (13 species), we find that for an average fish, the optimum growth

252   temperature declines as it grows in size. This finding emerges despite the small range of body sizes

253   used in the experiments (only 10% of observations are larger than 50% of maturation size) (*SI*

254   *Appendix,* Fig. S2). Individuals of such small relative size likely invest little energy in

255   reproduction, which suggests that physiological constraints at warmer temperatures contribute to

256   reduced growth performance of large compared to small fish, in addition to increasing investment

257   into reproduction (Barneche *et al.* 2018).

258   Translating results from experimental data to natural systems is challenging because maximal

259   feeding rates, unlimited food supply, lack of predation, and constant temperatures do not reflect

260   natural conditions, yet affect growth rates (Brett *et al.* 1969; Lorenzen 1996; Huey & Kingsolver

261   2019). In addition, total metabolic costs in the wild also include additional costs for foraging and

262   predator avoidance. It is, however, typically found and assumed that standard metabolic rate and

263   natural feeding levels are proportional to routine metabolic rate and maximum consumption rate,

264   respectively, and thus exhibit the same mass-scaling relationships (Kitchell *et al.* 1977; Neuenfeldt

265   *et al.* 2020). Intraspecific growth rates may not appear to be unimodally related to temperature

266   when measured over a temperature gradient across populations within a species (Denderen *et al.*

267   2020), because each population can be adapted to local climate conditions and thus display

268   different temperature optima. However, each population likely has a thermal optimum for growth,

269   which differs between individuals of different size. Hence, each population might have a unimodal

270   relationship with temperature that differs from other populations of the same species. This

271   highlights the importance of understanding the time scale of environmental change in relation to

272   that of immediate physiological responses, acclimation, adaptation and community reorganization

273   for the specific prediction about climate change impacts. In natural systems, climate warming may

274   also result in stronger food limitation (Ohlberger *et al.* 2011; Huey & Kingsolver 2019). Hence,

275   as optimum growth temperatures decline not only with size but also food availability (Brett *et al.*

276   1969; Brett 1971), and realized consumption rates are a fraction of the maximum consumption rate

277   (20-70%) (Kitchell *et al.* 1977; Neuenfeldt *et al.* 2019), species may be negatively impacted by

278   warming even when controlled experiments show they can maintain growth capacity at these

279   temperatures. Supporting this point is the observation that warming already has negative or lack

280   of positive effects on body growth in populations living at the edge of their physiological tolerance

281   in terms of growth (Neuheimer *et al.* 2011; Huss *et al.* 2019).

282   Whether the largest fish of a population will be the first to experience negative effects of

283   warming, as suggested by the finding that optimum growth temperature declines with body size,

284   depends on the environmental temperatures they typically experience compared to smaller

285   conspecifics. For instance, large fish may inhabit colder temperatures compared to small fish due

286   to ontogenetic habitat shifts (Werner & Hall 1988; Lloret-Lloret *et al.* 2020); see also Heincke's

287   law (Heincke 1913; Audzijonyte & Pecl 2018). Yet, there is already empirical evidence of the

288   largest individuals in natural populations being the first to suffer from negative impacts of warming

289   from heatwaves (Pörtner & Knust 2007), or not being able to benefit from warming (Huss *et al.*

290   2019; Van Dorst *et al.* 2019). Hence, assuming that warming affects all individuals of a population

291   equally is a simplification that can bias predictions of the biological impacts of climate change.

292   The interspecific scaling of fundamental ecological processes with body mass and temperature

293   has been used to predict the effects of warming on body size, size structure, and population and

294   community dynamics (Vasseur & McCann 2005; Morita *et al.* 2010; Cheung *et al.* 2013; Gilbert

295   *et al.* 2014). We argue that a contributing factor to the discrepancy between mechanistic growth

296   models, general scaling theory, and empirical data has been the lack of data synthesis at the

297   intraspecific level. The approach presented here can help overcome limitations of small data sets

298   by borrowing information across species in a single modelling framework, while accounting for

299   the intraspecific scaling of rates. Accounting for the faster increase in whole-organism metabolism

300   than consumption with body size, the unimodal thermal response of consumption, and resulting

301   size-dependence of optimum growth temperatures is essential for understanding what causes

302   observed growth responses to global warming. Acknowledging these mechanisms is also

303   important for improving predictions on the consequences of warming effects on fish growth for

304   food web functioning, fisheries yields and global food production in warmer climates.

305

Materials and methods

Data acquisition

308   We searched the literature for experimental studies evaluating the temperature response of

309   individual maximum consumption rate (feeding rate at unlimited food supply, *ad libitum*), resting,

310   routine and standard oxygen consumption rate as a proxy for metabolic rate (Nelson 2016) and

311   growth rates across individuals of different sizes within species. We used three different searches

312   on the Web of Science Core Collection (see *SI Appendix*, for details). In order to estimate how

313   these rates depend on body size and temperature within species, we selected studies that

314   experimentally varied both body size and temperature (at least two temperature treatments and at

315   least two body masses). The average number of unique temperature treatments (temperature

316   rounded to nearest °C) by species is 7.2 for growth and 4.3 for consumption and metabolism data.

317   The criteria for both mass and temperature variation in the experiments reduce the number of

318   potential data sets, as most experimental studies use either size or temperature treatments, not both.

319   However, these criteria allow us to fit multiple regression models and estimate the effects of mass

320   and temperature jointly, and to evaluate the probability of interactive mass- and temperature effects

321   within species. Following common practice we excluded larval studies, which represents a life

322   stage exhibiting different constraints and scaling relationships than non-larval life stages (Glazier

323   2005).

324   Studies were included if (i) a unique experimental temperature was recorded for each trial

325   (±1°C), (ii) fish were provided food at *ad libitum* (consumption and growth data) or if they were

326   unfed (resting, standard or routine metabolic rate), and (iii) fish exhibited normal behavior during

327   the experiments. We used only one study per species and rate to ensure that all data within a given

328   species are comparable as measurements of these rates can vary between studies due to e.g.

329   measurement bias, differences in experimental protocols, or because different populations were

330   studied (Armstrong & Hawkins 2008; Jerde *et al.* 2019). In cases where we found more than one

331   study for a given rate and species, we selected the most suitable study based on our pre-defined

332   criteria (for details, see *SI Appendix*). We ensured that the experiments were conducted at

333   ecologically relevant temperatures (*SI Appendix,* Figs. S1, S3). A more detailed description of the

334   search protocol, data selection, acquisition, quality control, collation of additional information and

335   standardizing of rates to common units can be found in *SI Appendix*.

336   We compiled four datasets: maximum consumption rate, metabolic rate, growth rate and the

337   optimum growth temperature for each combination of body mass group and species. We compiled

338   a total of 746 measurements of maximum consumption rate (of which 666 are below peak), 2699

339   measurements of metabolic rate and 227 measurements of growth rate (45 optimum temperatures)

340   from published articles for each rate, from 20, 34 and 13 species, respectively, from different

341   taxonomic groups, habitats and lifestyles (Table S1-S2). We requested original data from all

342   corresponding authors of each article. In cases where we did not hear from the corresponding

343   author, we extracted data from tables or figures using Web Plot Digitizer (Rohatgi 2012).

344

345 **Model fitting**

346 *Model description*

347 To each dataset, we fit hierarchical models with different combinations of species-varying

348 coefficients, meaning they are estimated with shrinkage. This reduces the influence of outliers

349 which could occur in species with small samples sizes (Gelman & Hill 2007; Harrison *et al.* 2018).

350 The general form of the model is:

$$y_{ij} \sim N(\mu_{ij}, \sigma) \tag{1}$$

351

$$\mu_{ij} = \beta_{0j} + \sum_{p=1}^{n}(\beta_p \times x_{ip}) \tag{2}$$

352

$$\beta_{0j} \sim N(\mu_{\beta_0}, \sigma_{\beta_0}) \tag{3}$$

353

354 where y_{ij} is the ith observation for species j for rate y, β_{0j} is a species-varying intercept, x_{ip} is a

355 predictor and β_p is its coefficient, with $p = 1, \ldots n$, where n is the number of predictors considered

356 in the model (mass, temperature, and their interaction). Predictors are mean centered to improve

357 interpretability (Schielzeth 2010). Species-level intercepts follow a normal distribution with

358 hyperparameters μ_{β_0} (global intercept) and σ_{β_0} (between-species standard deviation). For most

359 models we also allow the coefficient β_p to vary between species, such that β_p becomes β_{pj} and

360 x_{ip} x_{ijp}, where $\beta_{pj} \sim N(\mu_{\beta_p}, \sigma_{\beta_p})$. For each dataset, we evaluate multiple combinations of species-

361 varying coefficients (from varying intercept to n varying coefficients). We used a mix of flat,

362 weakly informative, and non-informative priors. For the temperature and mass coefficients we

363 used the predictions from the MTE as the means of the normal prior distributions (Brown *et al.*

364 2004), but with large standard deviations (see *SI Appendix*, Table S3). Below we describe how the

365 model in Eqns. 1-3 is applied to each data set.

366

367   *Mass- and temperature dependence of consumption, metabolism and growth below peak*

368   *temperatures*

369   Peak temperature (optimum in the case of growth) refers to the temperature at which the rate was

370   maximized, by size group. For data below peak temperatures, we assumed that maximum

371   consumption rate, metabolism and growth scale allometrically (as a power function of the form

372     $I = i_0 M^{b_0}$) with mass, and exponentially with temperature. Hence, after log-log (natural log)

373   transformation of mass and the rate, and temperature in Arrhenius temperature ($1/kT$ in unit eV^{-1},

374   where k is Boltzmann's constant [8.62×10^{-5} eV K^{-1}]), the relationship between the rate and its

375   predictors becomes linear. This is similar to the MTE, except that we estimate all coefficients

376   instead of correcting rates, and allow not only the intercepts but also slopes to vary across species.

377   When applied to Eqns. 1-3, y_{ij} is the ith observation for species j of the natural log of the rate

378   (consumption, metabolism or growth), and the predictors are m_{ij} (natural log of body mass), $t_{A,ij}$

379   (Arrhenius temperature, $1/kT$ in unit eV^{-1}), both of which were mean-centered, and their

380   interaction. Body mass is in g, consumption rate in g day^{-1}, metabolic rate in mg O_2 h^{-1} and

381   specific growth rate in unit % day^{-1}. We use resting or routine metabolism (mean oxygen uptake

382   of a resting unfed fish only showing some spontaneous activity) and standard metabolism (resting

383   unfed and no activity, usually inferred from extrapolation or from low quantiles of routine

384   metabolism, e.g. lowest 10% of measurements) to represent metabolic rate (Beamish 1964;

385   Ohlberger *et al.* 2007). Routine and resting metabolism constitute 58% of the data used and

386   standard metabolism constitutes 42%. We accounted for potential differences between these types

387   of metabolic rate measurements by adding two dummy coded variables, $type_r$ and $type_s$, the

388   former taking the value 0 for standard and 1 for a routine or resting metabolic rate measurement,

389   and vice versa for the latter variable. Thus, for metabolism, we replace the overall intercept β_{0j} in

390   Eqns. 2-3 with β_{0rj} and β_{0sj}. β_{0sj} is forced to 0 for a species that has a routine or resting metabolic

391   rate and β_{0rj} is forced to 0 for a species with standard metabolic rate data. We assume these

392   coefficients vary by species following normal distributions with global means $\mu_{\beta_{0r}}$ and $\mu_{\beta_{0s}}$, and

393   standard deviations $\sigma_{\beta_{0r}}$ and $\sigma_{\beta_{0s}}$, i.e. $\beta_{0rj} \sim N(\mu_{\beta_{0r}}, \sigma_{\beta_{0r}})$ and $\beta_{0sj} \sim N(\mu_{\beta_{0s}}, \sigma_{\beta_{0s}})$.

394

395   *Mass- and temperature dependence of consumption including beyond peak temperatures*

396   Over a large temperature range, many biological rates are unimodal. We identified such tendencies

397   in 10 out of 20 species in the consumption data set. To characterize the decline in consumption

398   rate beyond peak temperature, we fit a mixed-effects version of the Sharpe Schoolfield equation

399   (Schoolfield *et al.* 1981) as expressed in (Padfield *et al.* 2020), to equations 1-2 with y_{ij} as rescaled

400   consumption rates (C). Specifically, we model μ_{ij} in Eq. 1 with the Sharpe-Schoolfield equation:

401
$$\mu_{ij} = \frac{C_{0j}(T_C)e^{E_j\left(\frac{1}{kT_C}-\frac{1}{kT}\right)}}{1+e^{E_h\left(\frac{1}{kT_h}-\frac{1}{kT}\right)}} \tag{4}$$

402
$$E_j \sim N(\mu_E, \sigma_E) \tag{5}$$

403
$$C_{0j} \sim N(\mu_{C_0}, \sigma_{C_0}) \tag{6}$$

404   where $C_{0j}(T_C)$ is the rate at a reference temperature T_C in Kelvin [K] (here set to 263.15), E_j [eV]

405   is the activation energy, E_h [eV] characterizes the decline in the rate past the peak temperature and

406   T_h [K] is the temperature at which the rate is reduced to half (of the rate in the absence of

407   deactivation) due to high temperatures. We assume E_j and C_{0j} vary across species according to a

408   normal distribution with means μ_E and μ_{C_0}, and standard deviations σ_E and σ_{C_0} (Eq. 5-6). Prior to

409   rescaling maximum consumption (in unit g day^{-1}) by dividing $C_{i,j}$ with the mean within species

410    $\overline{C}_j$, we isolate the effect of mass by dividing consumption with $m^{0.63}$, which is the estimated

411   allometric relationship from the log-linear model. Temperature, T, is centered by subtracting the

412   temperature at peak consumption. This was estimated separately for each species using the Sharpe-

413   Schoolfield equation but without group-varying coefficients in a frequentist framework (see

414   '*Parameter estimation*'). The rescaling is done to control for differences in the optimum

415   temperature between species, which if not accounted for obscures the average relationship between

416   consumption and temperature among species.

417

418   *Mass-dependence of optimum growth temperature*

419   To evaluate how the optimum temperature ($t_{opt,ij}$, in degrees Celsius) for individual growth

420   depends on body mass, we fit Eqns. 1-3 with y_{ij} as the mean-centered optimum growth

421   temperature within species ($t_{opt,ij} = T_{opt,ij} - \bar{T}_{opt,j}$), to account for species being adapted to

422   different thermal regimes. m_{ij}, the predictor variable for this model, is the natural log of the ratio

423   between mass and mass at maturation acquired from FishBase (Froese & Pauly 2019), within

424   species: $m_{ij} = \ln(M_{ij}/M_{mat,j}) - \overline{\ln(M_{ij}/M_{mat,j})}$. This rescaling is done because we are

425   interested in examining relationships within species over "ontogenetic size", and because we do

426   not expect an interspecific relationship between optimum growth temperature and body mass

427   because species are adapted to different thermal regimes. We consider both the intercept and the

428   effect of mass to potentially vary between species.

429

430   *Parameter estimation*

431   We fit the models in a Bayesian framework, using R version 4.0.2 (R Core Team 2020) and JAGS

432   (Plummer 2003) through the R-package '*rjags*' (Plummer 2019). We used 3 Markov chains with

433   5000 iterations for adaptation, followed by 15000 iterations burn-in and 15000 iterations sampling

434   where every 5th iteration saved. Model convergence was assessed by visually inspecting trace plots

435   and potential scale reduction factors ($\hat{R}$) (*SI Appendix*). $\hat{R}$ compares chain variance with the pooled

436   variance, and values <1.1 suggest all three chains converged to a common distribution (Gelman *et*

437   *al.* 2003). We relied heavily on the R packages within '*tidyverse*' (Wickham *et al.* 2019) for data

438   processing, as well as '*ggmcmc*' (Fernández-i-Marín 2016), '*mcmcviz*' (Youngflesh 2018) and

439   '*bayesplot*' (Gabry *et al.* 2019) for visualization. Single-species Sharpe-Schoolfield models were

440   fitted using the packages '*rTPC*' (Padfield & O'Sullivan 2020) and '*nls.multstart*' (Padfield &

441   Matheson 2020)

442

443   *Model comparison*

444   We compared the parsimony of models with different hierarchical structures, and with or without

445   mass-temperature interactions, using the Watanabe-Akaike information criterion (WAIC)

446   (Watanabe 2013; Vehtari *et al.* 2017), which is based on the posterior predictive distribution. We

447   report WAIC for each model descried above (Table S4-S5), and examine models with ΔWAIC

448   values < 2, where ΔWAIC is each models difference to the lowest WAIC across models, in line

449   with other studies (Olmos *et al.* 2019).

450

451   *Net energy gain*

452   The effect of temperature and mass dependence of maximum consumption and metabolism

453   (proportional to biomass gain and losses, respectively) (Ursin 1967; Kitchell *et al.* 1977; Essington

454   *et al.* 2001) on growth is illustrated by visualizing the net energy gain. The model for the net energy

455   gain (growth) can be viewed as an empirical temperature-dependent Pütter-type model. Pütter-

456   type models are the simplest growth models based on a dynamic energy budget, and make strong

457   assumptions about mass-scaling of key life-history and physiological processes (e.g., maturation

458   and assimilation). However, Pütter-type models are among the most commonly applied growth

459   models in ecology and fisheries, they tend to fit data reasonably well (Marshall & White 2019),

460   and are suitable for illustrating the consequences of non-linear consumption rates due to their

461   simplicity (in contrast to more complex and parameter-rich dynamic energy budget models, e.g.

462   (Kitchell *et al.* 1977; Cuenco *et al.* 1985)). A Pütter model is the result of two antagonistic

463   allometric processes, biomass gains and biomass losses:

$$\frac{dM}{dt} = H(T)M^a - K(T)M^b \tag{7}$$

465   where M is body mass and T is temperature, H and K the allometric constants and a and b the

466   exponents of the processes underlying gains and losses, respectively. We convert metabolism from

467   oxygen consumption [mg O_2 h^{-1} day^{-1}] to g day^{-1} by assuming 1 kcal = 295 mg O_2 (based on

468   an oxycaloric coefficient of 14.2 J/mg O_2) (Hepher 1988), 1 kcal = 4184 J and an energy content

469   of 5600 J/g (wet weight) (Rijnsdorp & Ibelings 1989). Consumption rate is already in unit g day^{-1}.

470   Consumption and metabolic rates are calculated for two sizes (5 and 1000 g, which roughly

471   correspond to the 25th percentile of both datasets and the maximum mass in the consumption data,

472   respectively), using the global allometric relationships found in the log-log models fit to sub-peak

473   temperatures. These allometric functions are further scaled with the temperature correction factors

474   r_c for consumption and r_m for metabolism. r_c is based on the Sharpe-Schoolfield model and r_m is

475   given by the temperature dependence of metabolic rate from the log-linear model. Because r_c and

476   r_m are fitted to data on different scales, we divide these functions by their maximum. Lastly, we

477   rescale the product between the allometric functions and r_c and r_m such that the rate at 19°C (mean

478   temperature in both data sets) equals the temperature-independent rate.

479

Acknowledgements

Author contributions

ML conceived the study; ML, JO, AG designed research; ML performed research with input from JO and AG; ML, JO, AG wrote the paper and contributed to revisions of the manuscript.

Data accessibility statement

All data and R code (lists of studies in literature search, data preparation, analyses and figures) can be downloaded from a GitHub repository (https://github.com/maxlindmark/scaling) and will be archived on Zenodo upon publication.

References

Andersen, K.H., Beyer, J.E. & Lundberg, P. (2009). Trophic and individual efficiencies of size-structured communities. *Proceedings of the Royal Society B: Biological Sciences*, 276, 109–114.

Angilletta, M.J. & Dunham, A.E. (2003). The temperature-size rule in ectotherms: simple evolutionary explanations may not be general. *The American Naturalist*, 162, 332–342.

Armstrong, J.D. & Hawkins, L.A. (2008). Standard metabolic rate of pike, *Esox lucius*: variation among studies and implications for energy flow modelling. *Hydrobiologia*, 601, 83–90.

506 Atkinson, D. (1994). Temperature and organism size—A biological law for ectotherms? In:
507   *Advances in Ecological Research*. Elsevier, pp. 1–58.
508 Audzijonyte, A., Barneche, D.R., Baudron, A.R., Belmaker, J., Clark, T.D., Marshall, C.T., *et al.*
509   (2019). Is oxygen limitation in warming waters a valid mechanism to explain decreased
510   body sizes in aquatic ectotherms? *Global Ecology and Biogeography*, 28, 64–77.
511 Audzijonyte, A. & Pecl, G.T. (2018). Deep impact of fisheries. *Nature Ecology & Evolution*, 2,
512   1348–1349.
513 Audzijonyte, A., Richards, S.A., Stuart-Smith, R.D., Pecl, G., Edgar, G.J., Barrett, N.S., *et al.*
514   (2020). Fish body sizes change with temperature but not all species shrink with warming.
515   *Nat Ecol Evol*, 4, 809–814.
516 Barneche, D.R. & Allen, A.P. (2018). The energetics of fish growth and how it constrains food-
517   web trophic structure. *Ecology Letters*, 21, 836–844.
518 Barneche, D.R., Jahn, M. & Seebacher, F. (2019). Warming increases the cost of growth in a
519   model vertebrate. *Functional Ecology*, 33, 1256–1266.
520 Barneche, D.R., Robertson, D.R., White, C.R. & Marshall, D.J. (2018). Fish reproductive-energy
521   output increases disproportionately with body size. *Science*, 360, 642–645.
522 Baudron, A.R., Needle, C.L., Rijnsdorp, A.D. & Marshall, C.T. (2014). Warming temperatures
523   and smaller body sizes: synchronous changes in growth of North Sea fishes. *Global
524   Change Biology*, 20, 1023–1031.
525 Beamish, F.W.H. (1964). Respiration of fishes with special emphasis on standard oxygen
526   consumption II. Influence of weight and temperature on respiration of several species'.
527   *Canadian Journal of Zoology/Revue Canadienne de Zoologie*, 42, 177–188.
528 von Bertalanffy, L. (1957). Laws in metabolism and growth. *The quarterly review of biology*, 32,
529   217–231.
530 Björnsson, B., Steinarsson, A. & Árnason, T. (2007). Growth model for Atlantic cod (*Gadus
531   morhua*): Effects of temperature and body weight on growth rate. *Aquaculture*, 271, 216–
532   226.
533 Blanchard, J.L., Heneghan, R.F., Everett, J.D., Trebilco, R. & Richardson, A.J. (2017). From
534   bacteria towWhales: Using functional size spectra to model marine ecosystems. *Trends in
535   Ecology & Evolution*, 32, 174–186.
536 Bokma, F. (2004). Evidence against universal metabolic allometry. *Functional Ecology*, 18,
537   184–187.
538 Brett, J.R. (1971). Energetic responses of salmon to temperature. A study of some thermal
539   relations in the physiology and freshwater ecology of sockeye salmon (*Oncorhynchus
540   nerka*). *Integr Comp Biol*, 11, 99–113.
541 Brett, J.R., Shelbourn, J.E. & Shoop, C.T. (1969). Growth rate and body composition of
542   fingerling sockeye salmon, *Oncorhynchus nerka*, in relation to temperature and ration
543   size. *J. Fish. Res. Bd. Can.*, 26, 2363–2394.
544 Brown, J.H., Gillooly, J.F., Allen, A.P., Savage, V.M. & West, G.B. (2004). Toward a metabolic
545   theory of ecology. *Ecology*, 85, 1771–1789.
546 Cheung, W.W.L., Sarmiento, J.L., Dunne, J., Frölicher, T.L., Lam, V.W.Y., Deng Palomares,
547   M.L., *et al.* (2013). Shrinking of fishes exacerbates impacts of global ocean changes on
548   marine ecosystems. *Nature Climate Change*, 3, 254–258.
549 Clarke, A. & Johnston, N.M. (1999). Scaling of metabolic rate with body mass and temperature
550   in teleost fish. *Journal of Animal Ecology*, 68, 893–905.

551 Cuenco, M.L., Stickney, R.R. & Grant, W.E. (1985). Fish bioenergetics and growth in
552   aquaculture ponds: I. Individual fish model development. *Ecological Modelling*, 27, 169–
553   190.
554 Daufresne, M., Lengfellner, K. & Sommer, U. (2009). Global warming benefits the small in
555   aquatic ecosystems. *Proceedings of the National Academy of Sciences, USA*, 106, 12788–
556   12793.
557 Dell, A.I., Pawar, S. & Savage, V.M. (2011). Systematic variation in the temperature dependence
558   of physiological and ecological traits. *Proceedings of the National Academy of Sciences*,
559   108, 10591–10596.
560 Denderen, D. van, Gislason, H., Heuvel, J. van den & Andersen, K.H. (2020). Global analysis of
561   fish growth rates shows weaker responses to temperature than metabolic predictions.
562   *Global Ecology and Biogeography*, 29, 2203–2213.
563 Downs, C.J., Hayes, J.P. & Tracy, C.R. (2008). Scaling metabolic rate with body mass and
564   inverse body temperature: A test of the Arrhenius fractal supply model. *Functional*
565   *Ecology*, 22, 239–244.
566 Elliott, J.M. & Hurley, M.A. (1995). The functional relationship between body size and growth
567   rate in fish. *Functional Ecology*, 9, 625.
568 Englund, G., Öhlund, G., Hein, C.L. & Diehl, S. (2011). Temperature dependence of the
569   functional response. *Ecology Letters*, 14, 914–921.
570 Essington, T.E., Kitchell, J.F. & Walters, C.J. (2001). The von Bertalanffy growth function,
571   bioenergetics, and the consumption rates of fish. *Canadian Journal of Fisheries and*
572   *Aquatic Sciences*, 58, 2129–2138.
573 Fernández-i-Marín, X. (2016). ggmcmc: Analysis of MCMC Samples and Bayesian Inference.
574   *Journal of Statistical Software*, 70, 1–20.
575 Forster, J., Hirst, A.G. & Atkinson, D. (2012). Warming-induced reductions in body size are
576   greater in aquatic than terrestrial species. *PNAS*, 109, 19310–19314.
577 Froese, R. & Pauly, D. (2019). *Editors. FishBase*. World Wide Web electronic publication.
578   www.fishbase.org, (12/2019).
579 Fussmann, K.E., Schwarzmüller, F., Brose, U., Jousset, A. & Rall, B.C. (2014). Ecological
580   stability in response to warming. *Nature Climate Change*, 4, 206–210.
581 Gabry, J., Simpson, D., Vehtari, A., Betancourt, M. & Gelman, A. (2019). Visualization in
582   Bayesian workflow. *J. R. Stat. Soc. A*, 182, 389–402.
583 García García, B., Cerezo Valverde, J., Aguado-Giménez, F., García García, J. & Hernández,
584   M.D. (2011). Effect of the interaction between body weight and temperature on growth
585   and maximum daily food intake in sharpsnout sea bream (*Diplodus puntazzo*).
586   *Aquaculture International*, 19, 131–141.
587 Gardner, J.L., Peters, A., Kearney, M.R., Joseph, L. & Heinsohn, R. (2011). Declining body size:
588   a third universal response to warming? *Trends in Ecology & Evolution*, 26, 285–291.
589 Gelman, A., Carlin, J., Stern, H. & Rubin, D. (2003). *Bayesian Data Analysis. 2nd edition*.
590   Chapman and Hall/CRC, Boca Raton.
591 Gelman, A. & Hill, J. (2007). *Data Analysis Using Regression and Multilevel/Hierarchical*
592   *Models*. Cambridge University Press.
593 Gilbert, B., Tunney, T.D., McCann, K.S., DeLong, J.P., Vasseur, D.A., Savage, V.M., *et al.*
594   (2014). A bioenergetic framework for the temperature dependence of trophic interactions.
595   *Ecology Letters*, 17, 902–914.

596   Gillooly, J.F., Brown, J.H., West, G.B., Savage, V.M. & Charnov, E.L. (2001). Effects of size
597   and temperature on metabolic rate. *Science*, 2248-2251.
598   Glazier, D.S. (2005). Beyond the "3/4-power law": variation in the intra- and interspecific
599   scaling of metabolic rate in animals. *Biological Reviews of the Cambridge Philosophical*
600   *Society*, 80, 611–662.
601   Handeland, S.O., Imsland, A.K. & Stefansson, S.O. (2008). The effect of temperature and fish
602   size on growth, feed intake, food conversion efficiency and stomach evacuation rate of
603   Atlantic salmon post-smolts. *Aquaculture*, 283, 36–42.
604   Harrison, X.A., Donaldson, L., Correa-Cano, M.E., Evans, J., Fisher, D.N., Goodwin, C.E.D., *et*
605   *al.* (2018). A brief introduction to mixed effects modelling and multi-model inference in
606   ecology. *PeerJ*, 6, e4794.
607   Hartvig, M., Andersen, K.H. & Beyer, J.E. (2011). Food web framework for size-structured
608   populations. *Journal of Theoretical Biology*, 272, 113–122.
609   Heincke, F. (1913). Rapp. Proc. Verb. Réun. ICES 16, 1–70.
610   Hepher, B. (1988). *Nutrition of Pond Fishes*. Cambridge University Press.
611   Horne, C.R., Hirst, Andrew.G. & Atkinson, D. (2015). Temperature-size responses match
612   latitudinal-size clines in arthropods, revealing critical differences between aquatic and
613   terrestrial species. *Ecology Letters*, 18, 327–335.
614   Huey, R.B. & Kingsolver, J.G. (2019). Climate warming, resource availability, and the metabolic
615   meltdown of ectotherms. *The American Naturalist*, 194, E140–E150.
616   Huss, M., Lindmark, M., Jacobson, P., Van Dorst, R.M. & Gårdmark, A. (2019). Experimental
617   evidence of gradual size-dependent shifts in body size and growth of fish in response to
618   warming. *Glob Change Biol*, 25, 2285–2295.
619   Ikpewe, I.E., Baudron, A.R., Ponchon, A. & Fernandes, P.G. (2020). Bigger juveniles and
620   smaller adults: Changes in fish size correlate with warming seas. *Journal of Applied*
621   *Ecology*, Early View.
622   Jerde, C.L., Kraskura, K., Eliason, E.J., Csik, S.R., Stier, A.C. & Taper, M.L. (2019). Strong
623   Evidence for an Intraspecific Metabolic Scaling Coefficient Near 0.89 in Fish. *Front.*
624   *Physiol.*, 10, 1166.
625   Jobling, M. (1997). Temperature and growth: modulation of growth rate via temperature change.
626   In: *Global Warming: Implications for Freshwater and Marine Fish* (eds. Wood, C.M. &
627   McDonald, D.G.). Cambridge University Press, Cambridge, pp. 225–254.
628   Kitchell, J.F., Stewart, D.J. & Weininger, D. (1977). Applications of a bioenergetics model to
629   yellow perch (*Perca flavescens*) and walleye (*Stizostedion vitreum vitreum*). *Journal of*
630   *the Fisheries Board of Canada*, 34, 1922–1935.
631   Kooijman, S.A.L.M. (1993). *Dynamic energy budgets in biological systems*. Cambridge
632   University Press.
633   Lefevre, S., McKenzie, D.J. & Nilsson, G.E. (2018). In modelling effects of global warming,
634   invalid assumptions lead to unrealistic projections. *Global Change Biology*, 24, 553–556.
635   Lemoine, N.P. & Burkepile, D.E. (2012). Temperature-induced mismatches between
636   consumption and metabolism reduce consumer fitness. *Ecology*, 93, 2483–2489.
637   Lindmark, M., Huss, M., Ohlberger, J. & Gårdmark, A. (2018). Temperature-dependent body
638   size effects determine population responses to climate warming. *Ecology Letters*, 21,
639   181–189.
640   Lindmark, M., Ohlberger, J., Huss, M. & Gårdmark, A. (2019). Size-based ecological
641   interactions drive food web responses to climate warming. *Ecology Letters*, 22, 778–786.

642   Lloret-Lloret, E., Navarro, J., Giménez, J., López, N., Albo-Puigserver, M., Pennino, M.G., *et al.*
643   (2020). The seasonal distribution of a highly commercial fish is related to ontogenetic
644   changes in its feeding strategy. *Front. Mar. Sci.*, 7.
645   Lorenzen, K. (1996). The relationship between body weight and natural mortality in juvenile and
646   adult fish: a comparison of natural ecosystems and aquaculture. *Journal of Fish Biology*,
647   49, 627–642.
648   Marshall, D.J. & White, C.R. (2019). Have we outgrown the existing models of growth? *Trends
649   in Ecology & Evolution*, 34, 102–111.
650   Maury, O. & Poggiale, J.-C. (2013). From individuals to populations to communities: A dynamic
651   energy budget model of marine ecosystem size-spectrum including life history diversity.
652   *Journal of Theoretical Biology*, 324, 52–71.
653   Morita, K., Fukuwaka, M., Tanimata, N. & Yamamura, O. (2010). Size-dependent thermal
654   preferences in a pelagic fish. *Oikos*, 119, 1265–1272.
655   Nelson, J.A. (2016). Oxygen consumption rate v. rate of energy utilization of fishes: a
656   comparison and brief history of the two measurements. *Journal of Fish Biology*, 88, 10–
657   25.
658   Neubauer, P. & Andersen, K.H. (2019). Thermal performance of fish is explained by an interplay
659   between physiology, behaviour and ecology. *Conserv Physiol*, 7.
660   Neuenfeldt, S., Bartolino, V., Orio, A., Andersen, K.H., Andersen, N.G., Niiranen, S., *et al.*
661   (2020). Feeding and growth of Atlantic cod (*Gadus morhua* L.) in the eastern Baltic Sea
662   under environmental change. *ICES Journal of Marine Science*, 77, 624–632.
663   Neuheimer, A.B., Thresher, R.E., Lyle, J.M. & Semmens, J.M. (2011). Tolerance limit for fish
664   growth exceeded by warming waters. *Nature Climate Change*, 1, 110–113.
665   Ohlberger, J. (2013). Climate warming and ectotherm body size – from individual physiology to
666   community ecology. *Functional Ecology*, 27, 991–1001.
667   Ohlberger, J., Edeline, E., Vollestad, L.A., Stenseth, N.C. & Claessen, D. (2011). Temperature-
668   driven regime shifts in the dynamics of size-structured populations. *The American
669   Naturalist*, 177, 211–223.
670   Ohlberger, J., Mehner, Thomas., Staaks, Georg. & Hölker, Franz. (2012). Intraspecific
671   temperature dependence of the scaling of metabolic rate with body mass in fishes and its
672   ecological implications. *Oikos*, 121, 245–251.
673   Ohlberger, J., Staaks, G. & Hölker, F. (2007). Effects of temperature, swimming speed and body
674   mass on standard and active metabolic rate in vendace (*Coregonus albula*). *Journal of
675   Comparative Physiology, B*, 177, 905–916.
676   Olmos, M., Payne, M.R., Nevoux, M., Prévost, E., Chaput, G., Pontavice, H.D., *et al.* (2019).
677   Spatial synchrony in the response of a long range migratory species (*Salmo salar*) to
678   climate change in the North Atlantic Ocean. *Global Change Biology*, 26, 1319–1337.
679   Padfield, D., Castledine, M. & Buckling, A. (2020). Temperature-dependent changes to host–
680   parasite interactions alter the thermal performance of a bacterial host. *The ISME Journal*,
681   14, 389–398.
682   Padfield, D., Lowe, C., Buckling, A., Ffrench-Constant, R., Jennings, S., Shelley, F., *et al.*
683   (2017). Metabolic compensation constrains the temperature dependence of gross primary
684   production. *Ecology Letters*, 20, 1250–1260.
685   Padfield, D. & Matheson, G. (2020). *nls.multstart: Robust Non-Linear regression using AIC
686   Scores*.
687   Padfield, D. & O'Sullivan, H. (2020). *rTPC: Functions for fitting thermal performance curves*.

688 Panov, V.E. & McQueen, D.J. (1998). Effects of temperature on individual growth rate and body
689   size of a freshwater amphipod, 76, 1107–1116.
690 Pauly, D. (2021). The gill-oxygen limitation theory (GOLT) and its critics. *Science Advances*, 7,
691   eabc6050.
692 Pauly, D. & Cheung, W.W.L. (2018a). On confusing cause and effect in the oxygen limitation of
693   fish. *Global Change Biology*, 24, e743–e744.
694 Pauly, D. & Cheung, W.W.L. (2018b). Sound physiological knowledge and principles in
695   modeling shrinking of fishes under climate change. *Global Change Biology*, 24, e15–e26.
696 Pawar, S., Dell, A.I., Savage, V.M. & Knies, J.L. (2016). Real versus Artificial Variation in the
697   Thermal Sensitivity of Biological Traits. *The American Naturalist*, 187, E41–E52.
698 Pawar, S., Dell, A.I., & Van M. Savage. (2012). Dimensionality of consumer search space drives
699   trophic interaction strengths. *Nature*, 486, 485–489.
700 Perrin, N. (1995). About Berrigan and Charnov's life-history puzzle. *Oikos*, 137–139.
701 Plummer, M. (2003). JAGS: A program for analysis of Bayesian graphical models using Gibbs
702   sampling. *Working Papers*, 8.
703 Plummer, M. (2019). *rjags*.
704 Pörtner, H.O. & Knust, R. (2007). Climate change affects marine fishes through the oxygen
705   limitation of thermal tolerance. *Science*, 315, 95–97.
706 Pütter, A. (1920). Studien über physiologische Ähnlichkeit VI. Wachstumsähnlichkeiten.
707   *Pflügers Arch.*, 180, 298–340.
708 R Core Team. (2020). *R: A Language and Environment for Statistical Computing. R Foundation
709   for Statistical Computing*. Vienna, Austria.
710 Rall, B.C., Brose, U., Hartvig, M., Kalinkat, G., Schwarzmuller, F., Vucic-Pestic, O., *et al.*
711   (2012). Universal temperature and body-mass scaling of feeding rates. *Philosophical
712   Transactions of the Royal Society of London, Series B: Biological Sciences*, 367, 2923–
713   2934.
714 Rall, B.C., Vucic-Pestic, O., Ehnes, R.B., Emmerson, M. & Brose, U. (2010). Temperature,
715   predator–prey interaction strength and population stability. *Global Change Biology*, 16,
716   2145–2157.
717 van Rijn, I., Buba, Y., DeLong, J., Kiflawi, M. & Belmaker, J. (2017). Large but uneven
718   reduction in fish size across species in relation to changing sea temperatures. *Global
719   Change Biology*, 23, 3667–3674.
720 Rijnsdorp, A.D. & Ibelings, B. (1989). Sexual dimorphism in the energetics of reproduction and
721   growth of North Sea plaice, Pleuronectes platessa L. *Journal of Fish Biology*, 35, 401–
722   415.
723 Rohatgi, A. (2012). *WebPlotDigitalizer: HTML5 based online tool to extract numerical data
724   from plot images. Version 4.1. [WWW document] URL
725   https://automeris.io/WebPlotDigitizer (accessed on January 2019)*.
726 de Roos, A.M. & Persson, L. (2001). Physiologically structured models – from versatile
727   technique to ecological theory. *Oikos*, 94, 51–71.
728 Savage, V.M., Gillooly, J.F., Brown, J.H., West, G.B. & Charnov, E.L. (2004). Effects of body
729   size and temperature on population growth. *The American Naturalist*, 163, 429–441.
730 Schielzeth, H. (2010). Simple means to improve the interpretability of regression coefficients:
731   Interpretation of regression coefficients. *Methods in Ecology and Evolution*, 1, 103–113.

732   Schoolfield, R.M., Sharpe, P.J.H. & Magnuson, C.E. (1981). Non-linear regression of biological
733   temperature-dependent rate models based on absolute reaction-rate theory. *Journal of*
734   *Theoretical Biology*, 88, 719–731.
735   Steinarsson, A. & Imsland, A.K. (2003). Size dependent variation in optimum growth
736   temperature of red abalone (*Haliotis rufescens*). *Aquaculture*, 224, 353–362.
737   Thresher, R.E., Koslow, J.A., Morison, A.K. & Smith, D.C. (2007). Depth-mediated reversal of
738   the effects of climate change on long-term growth rates of exploited marine fish.
739   *Proceedings of the National Academy of Sciences, USA*, 104, 7461–7465.
740   Uiterwaal, S.F. & DeLong, J.P. (2020). Functional responses are maximized at intermediate
741   temperatures. *Ecology*, 101, e02975.
742   Ursin, E. (1967). A Mathematical Model of Some Aspects of Fish Growth, Respiration, and
743   Mortality. *Journal of the Fisheries Research Board of Canada*, 24, 2355–2453.
744   Van Dorst, R.M., Gårdmark, A., Svanbäck, R., Beier, U., Weyhenmeyer, G.A. & Huss, M.
745   (2019). Warmer and browner waters decrease fish biomass production. *Global Change*
746   *Biology*, 25, 1395–1408.
747   Vasseur, D.A. & McCann, K.S. (2005). A mechanistic approach for modelling temperature-
748   dependent consumer-resource dynamics. *The American Naturalist*, 166, 184–198.
749   Vehtari, A., Gelman, A. & Gabry, J. (2017). Practical Bayesian model evaluation using leave-
750   one-out cross-validation and WAIC. *Stat Comput*, 27, 1413–1432.
751   Wang, H.-Y., Shen, S.-F., Chen, Y.-S., Kiang, Y.-K. & Heino, M. (2020). Life histories
752   determine divergent population trends for fishes under climate warming. *Nature*
753   *Communications*, 11, 4088.
754   Watanabe, S. (2013). A Widely Applicable Bayesian Information Criterion. *Journal of Machine*
755   *Learning Research*, 14, 867–897.
756   Werner, E.E. & Hall, D.J. (1988). Ontogenetic habitat shifts in bluegill: The foraging rate-
757   predation risk trade-off. *Ecology*, 69, 1352–1366.
758   Wickham, H., Averick, M., Bryan, J., Chang, W., D'Agostino McGowan, L., François, R., *et al.*
759   (2019). Welcome to the tidyverse. *Journal of Open Source Software*, 1686.
760   Wyban, J., Walsh, W.A. & Godin, D.M. (1995). Temperature effects on growth, feeding rate and
761   feed conversion of the Pacific white shrimp (*Penaeus vannamei*). *Aquaculture*, 138, 267–
762   279.
763   Xie, Xiaojun. & Sun, Ruyung. (1990). The Bioenergetics of the Southern Catfish (*Silurus*
764   *meridionalis* Chen). I. Resting Metabolic Rate as a Function of Body Weight and
765   Temperature. *Physiological Zoology*, 63, 1181–1195.
766   Youngflesh, C. (2018). MCMCvis: Tools to Visualize, Manipulate, and Summarize MCMC
767   Output. *Journal of Open Source Software*, 3, 640.
768

769 **Figures**

770
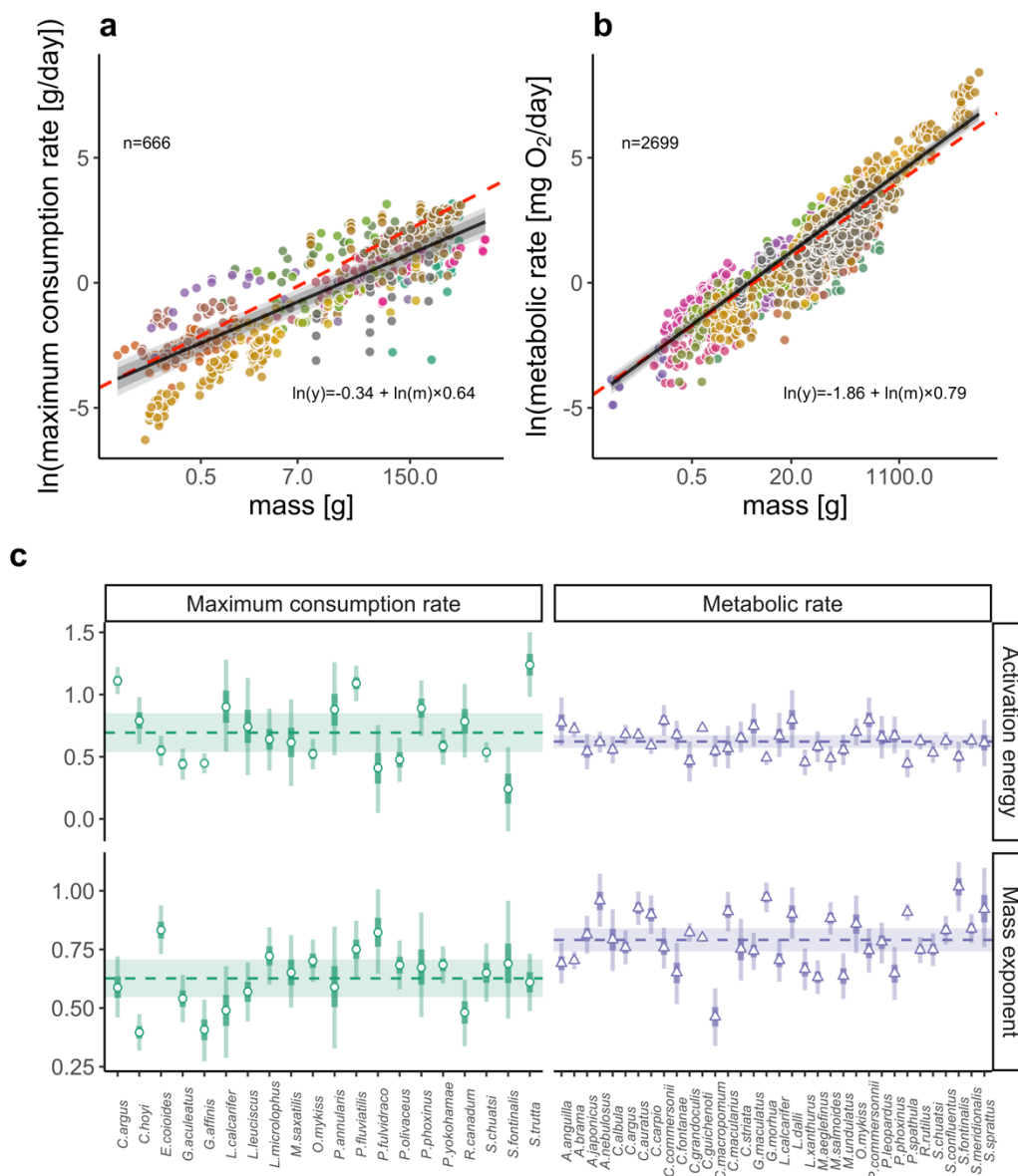
771 **Figure 1.** *Natural log of maximum consumption rate (A) and metabolic rate (B) against body mass*

772 *on a logarithmic x-axis. Lines are global predictions (routine metabolic rate in panel B) at the*

773 *average temperature in each data set (both 19°C, but note the model is fitted using mean-centred*

774 *Arrhenius temperature), hence the temperature terms are omitted. Red dahsed lines indicate a*

775 *slope of 3/4, corresponding to the prediction from the metabolic theory of ecology. Shaded areas*

776 *correspond to 80% and 95% credible intervals. Species are grouped by color (legend not shown,*

777　　*n=20 for consumption and n=34 for metabolism, respectively). C) Global and species-level effects*

778　　*of mass and temperature on maximum consumption rate and metabolic rate. Horizontal lines show*

779　　*the posterior medians of the global activation energies and mass exponents of maximum*

780　　*consumption and metabolism (μ_{β_1} and μ_{β_2} in Eqs. 6-8 for the mass and temperature coefficients,*

781　　*respectively). The shaded horizontal rectangles correspond to the posterior median $\pm$ 2 standard*

782　　*deviations. Points and triangles show the posterior medians for each species-level coefficient (for*

783　　*maximum consumption rate and metabolic rate, respectively), and the vertical bars show their*

784　　*80% and 95% credible interval.*

785
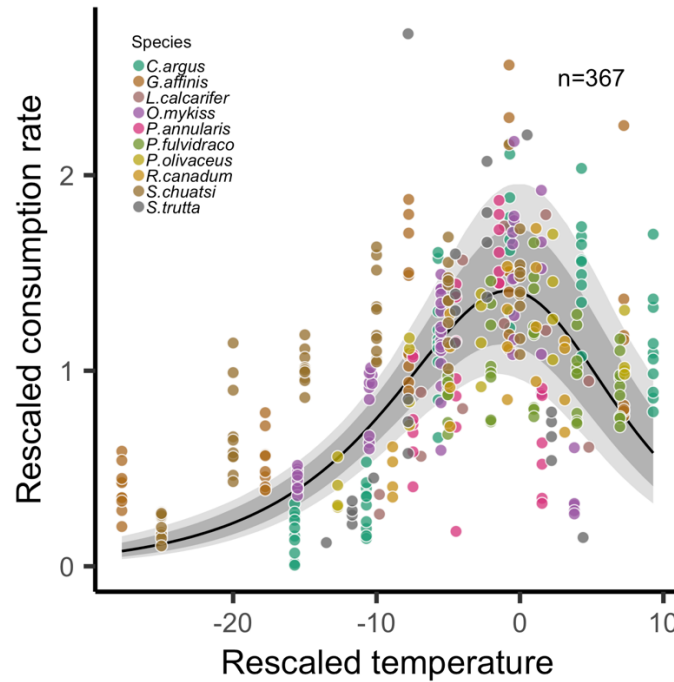
Figure 2. *Mass-corrected maximum consumption rate increases until a maximum is reached, after which it declines steeper than the initial rate of increase. Maximum consumption rates are relative to the average maximum consumption rates within species and temperature is the difference between the experimental temperature and the temperature where maximum consumption peaks (also by species). Lines show posterior median of predictions from the Sharpe-Schoolfield model (using the average intercept across species and the common coefficients), grey bands show 95% and 80% credible intervals. Colors indicate species.*
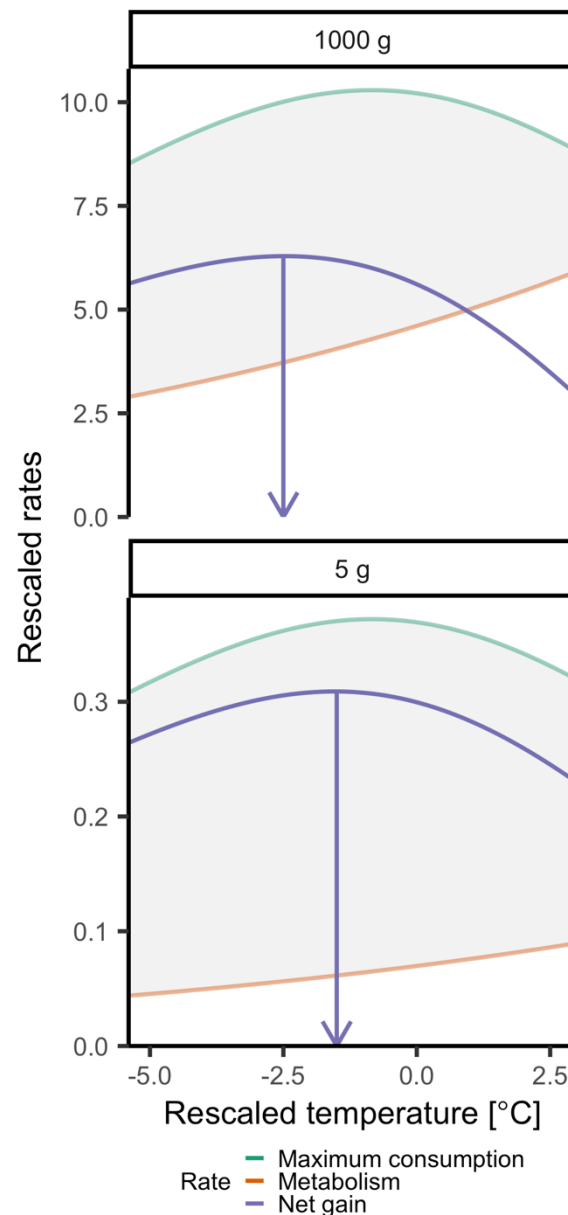
Figure 3. *Illustration of predicted whole-organism maximum consumption rate (green), metabolic rate (purple) and the difference between them (orange) for two body sizes (top=1000g, bottom=5g) (see ʹMaterials and Methodsʹ). Vertical arrows indicate the temperature where the difference in net energy gain (energy available for growth) is maximized for the two body sizes, which occurs at different temperatures despite that consumption peaks at the same temperature for both body sizes.*
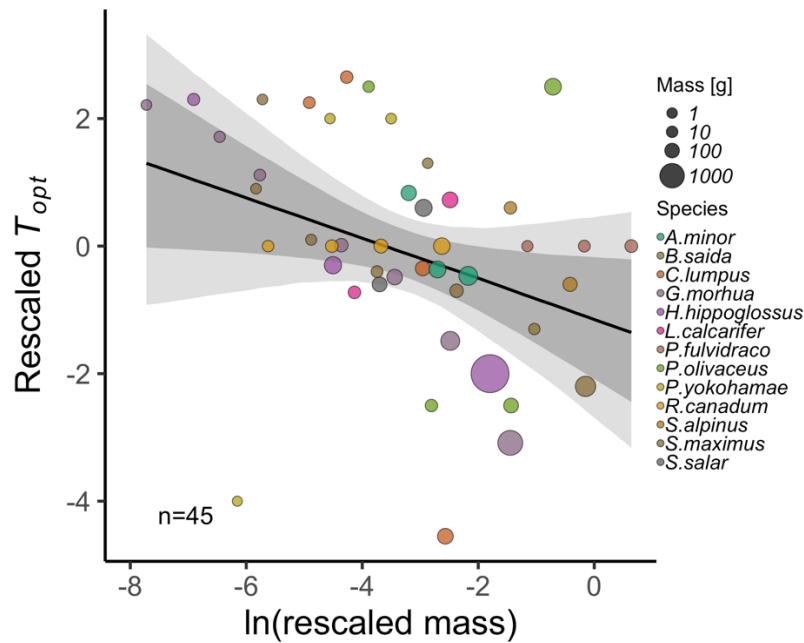
Figure 4. *Experimental data demonstrating optimum growth temperature declines with intraspecific body mass. The plot shows the optimum temperature within species (rescaled by subtracting the mean optimum temperature from each observation, by species) as a function of the natural log of rescaled body mass (ratio of mass to maturation mass within species). Probability bands represent 80% and 95% credible intervals, and the solid line shows the global prediction (μ_{β_0} and μ_{β_1}). Colors indicate species and the area of the circle corresponds to body mass in unit g.*